Rare Metal Materials and Engineering
Volume 51, Issue 6, June 2022
Available online at www.rmme.ac.cn

Science Press

Cite this article as: Qi Qian, Wang Lujie, Song Xiaojie. Oxidation Resistance Optimization of TiC/Hastelloy Composites by Designing Composition[J]. Rare Metal Materials and Engineering, 2022, 51(06): 1999-2004.

ARTICLE

Oxidation Resistance Optimization of TiC/Hastelloy Composites by Designing Composition

Qi Qian[1], Wang Lujie[2], Song Xiaojie[1]

[1] School of Materials Science and Engineering, Shandong University of Science and Technology, Qingdao 266590, China; [2] State Key Laboratory of Solid Lubrication, Lanzhou Institute of Chemical Physics, Chinese Academy of Sciences, Lanzhou 730000, China

Abstract: TiC/Hastelloy composite has been proposed as one of promising intermediate temperature solid oxide fuel cell interconnects, and the oxidation resistance is one key property for its application. TiC/Hastelloy composites with 50vol% and 58vol% metal matrix were prepared by reactive infiltration method. Results show that high metal content results in the increase in Cr content, which optimizes the oxidation resistance of TiC/Hastelloy composites by promoting formation of continuous Cr_2O_3 layer to inhibit external diffusion of Ni and Ti. The content of Ti and Ni oxides in oxide scale obviously decreases. The mass gain reduces from 2.03 to 0.55 mg·cm^{-2}. Meanwhile, in order to inhibit the migration of Cr, Co is extra introduced into the composites with 58vol% metal. During the oxidation process, Co and Fe (in metal matrix) show high external diffusion rate through Cr_2O_3, and generate in-situ $CoFe_2O_4$ layer outmost the oxide scale.

Key words: solid oxide fuel cell; interconnect; TiC/Hastelloy composites; oxidation resistance

Recently, some new kinds of intermediate temperature-solid oxide fuel cell (IT-SOFC) interconnects are proposed, such as TiC/Ni[1], TiC/FeAl[2], TiC/Ti_3Al[3] and Ti_3SiC_2 [4]. In comparison, TiC/Ni composites have many advantages, such as adjustable coefficient of thermal expansion (CTE), no insulating oxidation product (Al_2O_3 and SiO_2) and low cost. However, the oxidation resistance of TiC/Ni composites still needs to be improved. The lowest oxidation mass gain of composites reported was 0.5205 mg·cm^{-2} (800 °C/100 h, in air) with 10wt% Ni, and as Ni content increased to 20wt%, the mass gain of composites increased to 10.71 mg·cm^{-2} [5]. According to the request CTE (10.5×10^{-6}) of IT-SOFC interconnects and theoretical calculation of composites CTE (rule of mixture) [1], Ni content should be around 62wt% , which may lead to worse oxidation resistance of TiC/Ni composites. In contrast, the oxidation mass gain of Crofer 22 APU, which is generally used as IT-SOFC metallic interconnects, is only about 0.31 mg·cm^{-2} (800 °C/100 h, in air)[6]. Therefore, it is necessary to explore methods to optimize the oxidation resistance of TiC/Ni composites.

In our previous work, the oxidation process of TiC/Hastelloy composites was found to be controlled by external diffusion of Ni and Ti, and internal diffusion of O[7]. One effective method to improve the oxidation resistance of TiC/Hastelloy composites is to accelerate the formation of continuous TiO_2/Cr_2O_3 oxide scale by reducing interparticle spacing of TiC, thereby inhibiting the external diffusion of Ni and Ti[7,8]. Based on this result, the reasonable increase in Cr content may also promote the formation of continuous Cr_2O_3 layer to optimize the oxidation resistance of TiC/Hastelloy composites.

In addition, $CoFe_2O_4$ can effectively block the Cr migration, and some methods have been adopted to fabricate $CoFe_2O_4$ layer. Bi[9] prepared $CoFe_2O_4$ spinel layer on Crofer 22 APU ferritic steel via electroplating, in which $Co_{0.40}Fe_{0.60}$ alloy film was plated and then thermal converted into $CoFe_2O_4$ spinel coating. Yu[10] adopted the Fe and CoO powders as the precursor to form a dense $CoFe_2O_4$ layer on Crofer 22 APU by screen-printing and reactive sintering. Ebrahimifar[11] coated AISI 429 ferritic stainless steel with a cobalt-based layer using pack cementation, and the cobalt-based coating converted to Co_3O_4, $CoFe_2O_4$, and $CoCr_2O_4$ during oxidation exposure. In

Received date: June 14, 2021
Foundation item: Natural Science Foundation of Shandong Province (CN) (ZR2020QE003)
Corresponding author: Qi Qian, Ph. D., Lecturer, School of Materials Science and Engineering, Shandong University of Science and Technology, Qingdao 266590, P. R. China, Tel: 0086-532-80691739, E-mail: skd995891@sdust.edu.cn

this work, $CoFe_2O_4$ layer was also fabricated outmost the oxide scale of TiC/Hastelloy composites to inhibit the migration of Cr. Moreover, one simple method will be put forward. According to the high transport rate of Co and Fe through Cr_2O_3 [12], a small amount of Co is added into TiC/Hastelloy composites, which will react with Fe in Hastelloy to in-situ form $CoFe_2O_4$ layer outside Cr_2O_3.

In this study, TiC/Hastelloy composites with different Cr contents were fabricated by in-situ reactive infiltration method, and extra Co was introduced into the composites by adding Co particles in preform. The Cr content can be adjusted by changing the volume fraction of Hastelloy C-276, which contains 14.3wt% Cr. The microstructure of composites before and after oxidation process was compared and analyzed. The effect of Cr and Co content on the oxidation process of composites was studied.

1 Experiment

Graphite, Ti and Co particles (1 μm in diameter, 99.9% in purity, Haotian Nano Technology Co., Ltd, Shanghai, China) were used as raw materials. Hastelloy C-276 (Ni-based alloy, Hualong Special Steel Co., Ltd, Jiangsu, China) was metal matrix and the composition is provided in Table 1. The Cr content could be adjusted by changing metal matrix content. The fabrication process was carried out as follows. Firstly, Ti and graphite (Ti/C=1, in molar ratio) were ball-milled at 300 r/min in ethanol with titanium carbide media (ball to powder ratio, 1:1) for 4 h in a planetary mill, and then dried, crushed and sieved. There was no addition of Co to sample 1, while Co was added to sample 2. The contents of Co of sample 1 and 2 were 0.1wt% and 7.3wt%, respectively.

Secondly, the preform of samples was *Φ*45 mm×10 mm prepared by dry-pressing. The metal content in composites was altered by adjusting the mass of preform (Ti and graphite). Sample 2 was designed to have higher metal content (58vol%) than sample 1 (50vol%). Correspondingly, the Cr content increased from 9.2wt% (sample 1) to 10.2wt% (sample 2). Lastly, sufficient alloy ($m_{\text{alloy}} > \rho_{\text{alloy}} \cdot V_{\text{porosity of preform}}$) were laid above the preforms in alumina crucibles. The m_{alloy}, ρ_{alloy}, $V_{\text{porosity of preform}}$ means the mass of alloy, density of alloy and porosity of preforms, respectively. The infiltration was performed at 1450 °C for 0.5 h in argon atmosphere. In order to identify different samples in this study, samples 1 and 2 were labeled as TG and TG-C (composites with higher Cr and Co content).

The X-ray diffraction (XRD) Guinier-Hägg camera (Expectron XDC-1000, Jungner Instrument, Solna, Sweden) with Cu Kα radiation was used to test the phase composition of composites. The microstructure of composites before and after oxidation process was observed by scanning electron microscope (SEM, S-4800, HITACHI, Japan) equipped with an energy dispersive spectrometer (EDS). The density of the composites was tested by Archimedes' principle.

The CTE of composites were measured by NETZSCH Dilatometer 402C from 25 °C to 800 °C under air atmosphere. The four-probe method was adopted to measure the electrical resistivity using an IM6 electrochemical workstation (ZAHNER Germany) at 800 °C in air for 100 h. Weight was measured after 5, 10, 20, 30, 40, 50, 70 and 100 h. All the samples were subjected to isothermal oxidation at 800 °C in static air. Every sample was weighed before and after the oxidation by an electronic microbalance with an accuracy of 10^{-4} g. The samples for electrical resistivity, CTE and oxidation resistance tests were long bars with size of 36 mm×3 mm×4 mm, 20 mm×4 mm×4 mm and 20 mm×4 mm×4 mm, respectively. The samples were cut by electrical discharge machining.

2 Results and Discussion

2.1 Microstructure of composites

TiC/Hastelloy composites with high relative density (>95%) were prepared by in-situ reactive infiltration method, and their properties are shown in Table 2. Mo element in Hastelloy C-276 leads to the formation of core-rim structure of TiC particles[13], which are homogeneously distributed in metal matrix. Besides, the rim with different brightness, as shown in Fig.1c, is due to the higher Mo content. Because the atomic fraction of Mo is higher than that of Ti, the brightness increases as the Mo content increases in the rim. By comparing the microstructure of TG in Fig. 1a and TG-C in Fig. 1b, the higher metal matrix and Co content show no apparent effect on the formation of TiC particles. Moreover, according to the element composition of different points in Table 3, it can be seen that Co particles successfully dissolves into the metal matrix during infiltration process, which mainly exist in metal matrix of TG-C, as shown in Fig.1c.

2.2 Oxidation resistance of composites

The mass gain evolution of TG and TG-C in Fig. 2a as a function of holding time at 800 °C in air conforms to the parabolic kinetics law[14], described as following equation:

Table 1 Chemical composition of Hastelloy C-276 (wt%)

Ni	Cr	Fe	Mo	W	Co	Nb	Mn	Si	Al	Mg	Ti	Cu
62.6	14.3	5.1	12.3	4.0	0.18	0.04	0.46	0.44	0.25	0.04	0.14	0.15

Table 2 Properties of TG and TG-C samples

Samples	Metal content/vol%	Relative density/%	d_{TiC}/μm	Interparticles distance/μm	Mass gain/mg·cm^{-2}
TG	50	96.7	2.68	0.69	2.03
TG-C	58	97.8	2.61	0.88	0.55

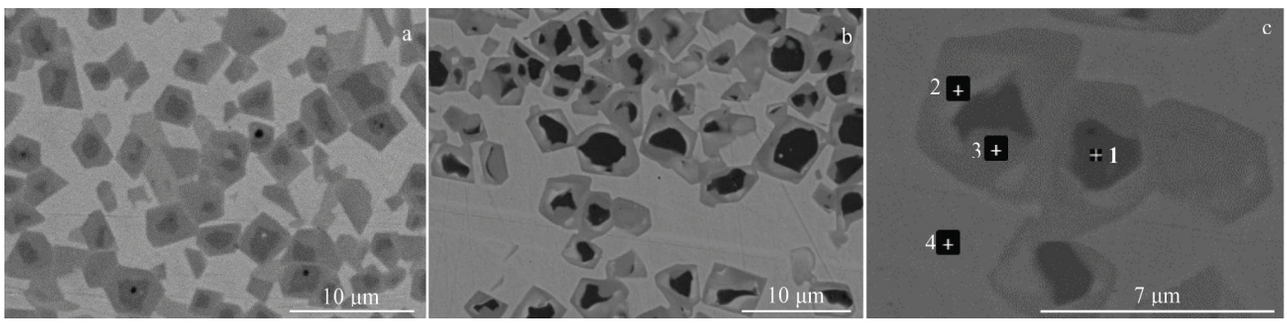

Fig.1 SEM micrographs of TG (a) and TG-C (b, c) composites

Table 3 Elements composition of different points marked in Fig.1c (at%)

Point	C	Ti	Mo	Ni	Cr	Co	Fe	W	Mn
1	56.80	41.48	0.96	0.44	0.18	-	-	0.14	-
2	67.23	17.27	10.52	1.38	1.63	-	-	1.98	-
3	68.70	19.42	8.51	1.13	1.03	-	-	1.21	-
4	-	1.85	4.89	67.76	18.13	1.64	4.97	-	0.76

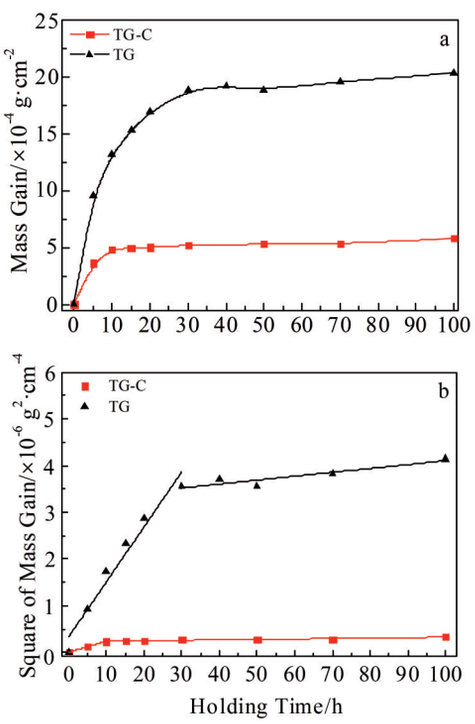

Fig.2 Mass gain (a) and square of mass gain (b) of composites TG and TG-C oxidized at 800 °C for 100 h in air

$$\left(\frac{\Delta W}{A}\right)^2 = kt \quad (1)$$

where ΔW, A, k and t mean the mass gain (mg), sample surface area (cm^2), parabolic rate constant (oxidation rate, $g^2 \cdot cm^{-4} \cdot h^{-1}$) and oxidation time (h), respectively. The mass gain of TG is 2.03 $mg \cdot cm^{-2}$, while the mass gain of TG-C is only 0.55 $mg \cdot cm^{-2}$. From Fig.2b, it can be seen that two stages exist in the oxidation process of TG and TG-C. As calculated by Eq.(1), the oxidation rate k of TG is 1.18×10^{-7} $g^2 \cdot cm^{-4} \cdot h^{-1}$ (0~30 h) and 8.35×10^{-9} $g^2 \cdot cm^{-4} \cdot h^{-1}$ (30~100 h), while the oxidation rate k of TG-C is 2.35×10^{-8} $g^2 \cdot cm^{-4} \cdot h^{-1}$ (0~10 h) and 0.97×10^{-9} $g^2 \cdot cm^{-4} \cdot h^{-1}$ (10~100 h), respectively. Thus, the increase of metal content in composites not only reduces mass gain and oxidation rate significantly, but also shrinks the first stage of oxidation process from 30 h to 10 h.

Fig.3 presents that the oxidation product of composites after oxidation for 100 h in air is complex, due to the multiple composition of Hastelloy C-276, as shown in Table 1. The main phases in oxide scale of TG are TiO_2, $NiTiO_3$, NiO and Fe_2O_3, while TiC/C_2MoTi, Ni-Cr, Cr_2O_3, $CoCr_2O_4$ and $CoFe_2O_4$ also appear in the oxide scale of TG-C. The strong peaks of TiC/C_2MoTi and Ni-Cr imply that the thinner oxide scale is formed on TG-C, and phases in composites under oxide scale can also be detected by X-ray.

To confirm the distributed location of oxidation products in oxide scale of TG and TG-C, the EDS mapping of different elements on the cross section of oxide scale is provided in Fig. 4. Firstly, the oxide scale on TG-C is much thinner than that of TG, consistent with the results of XRD in Fig.3, which demonstrates the better oxidation resistance of TG-C than TG. Secondly, the phase composition of oxide scale is also different between TG and TG-C. From Fig.4a to 4g, it can be obtained that from outside to inside of oxide scale of TG there are Ni+Fe+Ti, Ti and Cr oxides, respectively. According to the phase composition of oxide scale of TG in Fig. 3, it can be

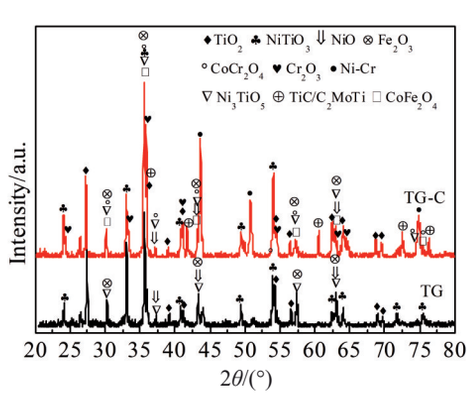

Fig.3 XRD patterns of composites TG and TG-C oxidized at 800 °C for 100 h in air

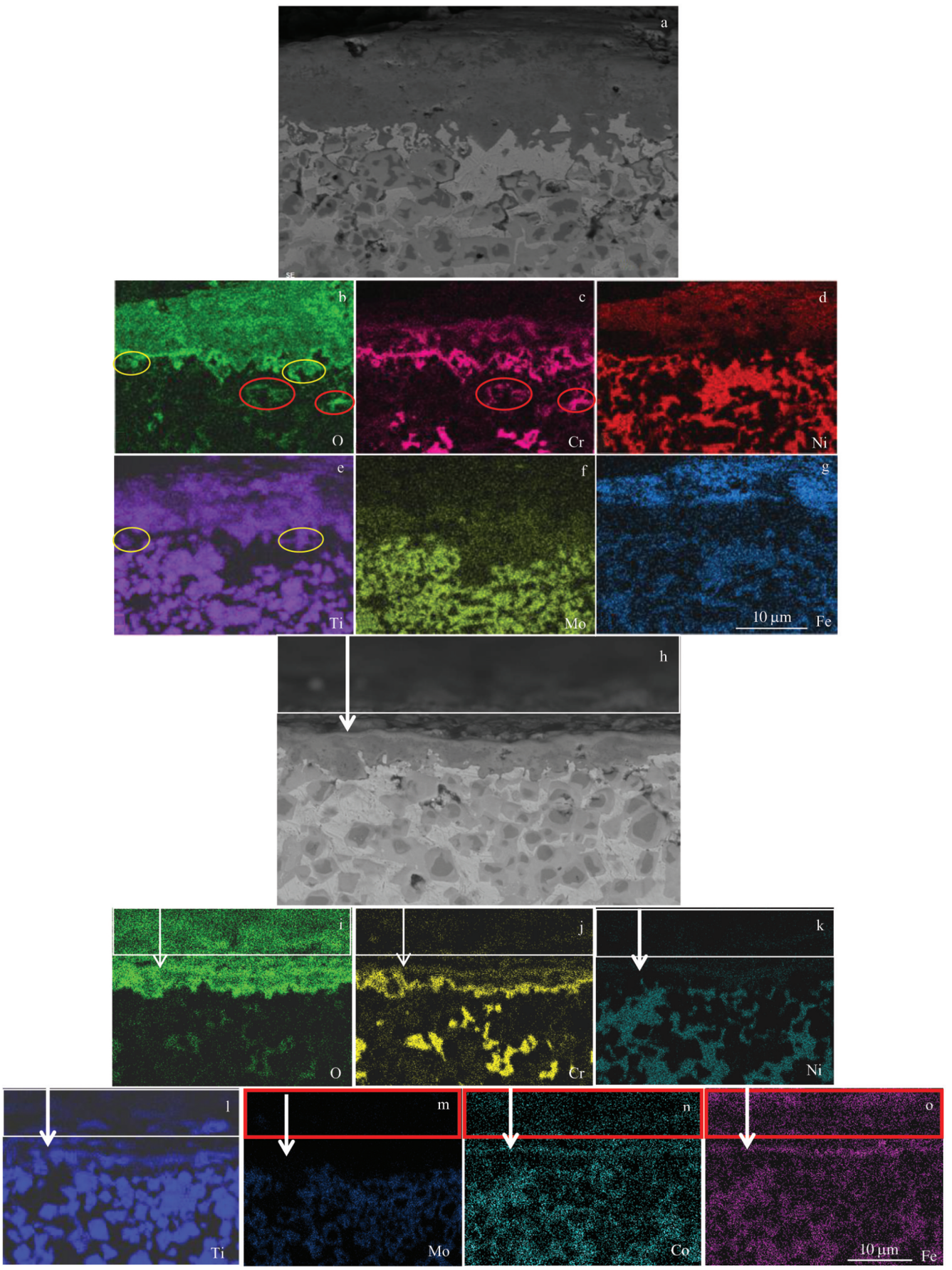

Fig.4 EDS mappings of O, Cr, Ni, Ti, Mo and Fe elements on the cross section of oxide scale of TG (a~g) and EDS mappings of O, Cr, Ni, Ti, Mo, Co and Fe elements on the cross section of selected oxide scale of TG-C oxidized at 800 °C for 100 h (h~o)

speculated that the oxide scale is mainly formed by NiO+$NiTiO_3$+TiO_2+Fe_2O_3/TiO_2/Cr_2O_3 with sandwich structure. Meanwhile, O internally diffuses and reacts with Cr and Ti to generate Cr_2O_3 and TiO_2 under the oxide scale, as pointed correspondingly by the red and yellow circles in Fig. 4b, 4c and 4e, in which the Cr or Ti and O elements coexist. By contrast, continuous Fe+Co+Cr, Ti and Cr oxides situate from outside to inside of oxide scale of TG-C, as shown in Fig. 4h~4o. In addition, as shown in Fig. 4h, the tested cross section was slightly sloping. The part higher than surface of tested cross section was surface of other part, as marked in the red box in Fig. 4h~4o. The major composition of the outmost part of oxide scale of TG-C is Co and Fe, while minute amount of Cr is still found in this layer, by comparing the EDS result of other surface in the red box. From the phase composition of oxide scale of TG-C in Fig. 3, it can be deduced that the oxide scale is mainly formed by $CoFe_2O_4$/TiO_2/Cr_2O_3 with sandwich structure. Furthermore, the increase in Co and Fe content would promote the formation of denser $CoFe_2O_4$ layer. The internal diffusion of O still exists in TG-C. However, Ni element is invisible in oxide scale, and the whole thickness of Ti and Cr oxides also decreases. Notably, the Cr_2O_3 layer in the oxide scale of TG-C is denser than that of TG, by comparing Fig. 4c and Fig. 4j. Besides, Mo element is mainly distributed in the substrate of TG and TG-C, and Mo-rich phase shows no obvious effect on the oxidation resistance of composites.

2.3 Thermal expansion and electrical conductivity of composites

As shown in Fig. 5, the increase of metal matrix content in TG-C results in higher CTE, 12.3×10^{-6} °C^{-1}, while the CTE of TG is 11.2×10^{-6} °C^{-1}. This coincides to the rule of mixture[15], and more metal content with high CTE will obtain composites with higher CTE. Similarly, higher metal content with better electrical conductivity results in composites with higher electrical conductivity, and thin oxide scale on TG-C also contributes to the high electrical conductivity. Therefore, the electrical conductivity of TG-C oxidized at 100 °C for 100 h is 5795 S·cm^{-1}, while the electrical conductivity of TG is 5727 S·cm^{-1}. The CTE and electrical conductivity of TG and TG-C can meet the requirements of IT-SOFC interconnects.

2.4 Discussion

Based on above experimental results, the effect of increasing Cr and Co content on the oxidation process of TG will be analyzed in detail. In our previous study, it has been found that the increase in metal content can improve the oxidation resistance in TiC/Hastelloy composites. As the metal content increases from 47vol% to 50vol%, the mass gain (800 °C, 100 h) decreases from 2.60 mg·cm^{-2} to 2.03 mg·cm^{-2} [7,16]. Moreover, the addition of 7wt% Co will not obviously influence the oxidation resistance of Ni-Cr based alloy[17]. Besides, Co shows no effect on the oxidation process of TiC[18]. Therefore, the increase of Cr content exhibits major influence on the optimization of oxidation resistance of TiC/Hastelloy composites.

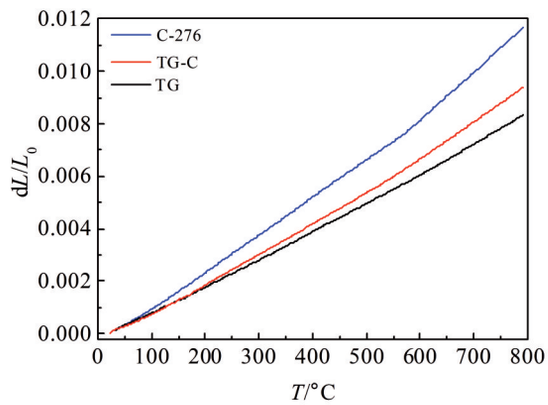

Fig.5 Thermal expansion curve of composites from 25 °C to 800 °C

As the volume fraction of metal matrix increases from 50% (TG) to 58% (TG-C), the interparticles spacing of TiC particles also increases from 0.69 μm to 0.88 μm, as shown in Table 2, and the calculation method has been described in the previous work[16]. The small interparticles spacing of TiC helps to the formation of continuous TiO_2 and Cr_2O_3 layer[8]. Beyond that, the Cr content also acts one key role in the fast formation of continuous Cr_2O_3 layer[19]. The final result is that the higher Cr content in TG-C, resulted from the high metal content, effectively promotes the fast formation of continuous Cr_2O_3 layer during oxidation process, leading to the shorter first stage. Besides, the Cr_2O_3 layer inhibits the external diffusion of Ni and Ti atoms, on the basis of disappearance of NiO and thinner TiO_2 layer outside the Cr_2O_3 layer, which contributes to the better oxidation resistance of TG-C. The time of the first stage of oxidation process shrinks from 30 h to 10 h, and mass gain decreases from 2.03 mg·cm^{-2} to 0.55 mg·cm^{-2}, while the oxidation rate k of stable period reduces from 8.35×10^{-9} $g^2\cdot cm^{-4}\cdot h^{-1}$ to 0.97×10^{-9} $g^2\cdot cm^{-4}\cdot h^{-1}$. In comparison, Co and Fe have high diffusion rate through Cr_2O_3, and continuous $CoFe_2O_4$ layer is in-situ formed at the outmost part of oxide scale of TG-C, as shown in Fig. 4n and Fig. 4o, which can restrain the chromium migration[9]. However, the content of Co should be further increased to form much dense $CoFe_2O_4$ layer, due to the slight Cr in it. Therefore, the increase of metal content in TiC/Hastelloy composites significantly optimizes their oxidation resistance, and the addition of Co leads to the in-situ formation of $CoFe_2O_4$ layer.

Moreover, the CTE of TG-C composites, Cr_2O_3, TiO_2 and $CoFe_2O_4$ are 12×10^{-6}, 9.6×10^{-6} [20], 9.0×10^{-6} [21] and 11.8×10^{-6} °C^{-1} [9], respectively. The difference of CTE will induce thermal stress during thermal cycle. However, the oxide scale spallation from composites is not found during oxidation, cutting and polishing process, as shown in the final sample in Fig. 4, which demonstrates the good adhesion of oxide scale to TG-C composites. Therefore, the metal content should be increased in a reasonable range to optimize the electrical conductivity and oxidation resistance of composites and meantime to insure the suitable CTE.

3 Conclusions

1) The TiC/Hastelloy composites with different metal and Co contents can be fabricated by in-situ reactive infiltration method.

2) Co particles dissolve into metal matrix during the infiltration process. High metal and Co content do not influence the formation of TiC particles with core-rim structure, while the oxidation resistance of composites is optimized notably.

3) High metal content leads to the increase in Cr content, which promotes the fast formation of continuous Cr_2O_3 layer to inhibit the external diffusion of Ni and Ti.

4) The time of the first stage of oxidation process shrinks from 30 h to 10 h, and mass gain decreases from 2.03 mg·cm^{-2} to 0.55 mg·cm^{-2}, while the oxidation rate k of stable period reduces from 8.35×10^{-9} g^2·cm^{-4}·h^{-1} to 0.97×10^{-9} g^2·cm^{-4}·h^{-1}. Meanwhile, Co and Fe show high diffusion rate through Cr_2O_3, and in-situ generate $CoFe_2O_4$ layer at the outside of oxide scale. Therefore, $CoFe_2O_4$ layer can be prepared by designing composition of composites.

References

1 Pang Y, Xie H, Koc R. *ECS Transactions*[J], 2007, 7(1): 2427

2 Tian L H, Li C X, Yang G J *et al*. *Journal of Power Sources*[J], 2013, 233: 394

3 Fu Z, Mondal K, Koc R. *Ceramics International*[J], 2016, 42(8): 9995

4 Zheng L, Hua Q, Li X *et al*. *International Journal of Hydrogen Energy*[J], 2018, 43(15): 7483

5 Koc R, Swift Geoffrey, Xie H. *Investigation of Novel Alloy TiC-Ni-Ni3Al for Solid Oxide Fuel Cell Interconnect Applications* [R]. US: Southern Illinois University at Carbondale, 2005

6 Ebrahimifar H, Zandrahimi M. *Oxidation of Metals*[J], 2015, 84(3-4): 329

7 Qi Q, Liu Y, Wang L J *et al*. *Journal of Power Sources*[J], 2017, 359: 626

8 Qi Q, Liu Y, Wang L J *et al*. *Journal of Power Sources*[J], 2017, 362: 57

9 Bi Z H, Zhu J H, Batey J L. *Journal of Power Sources*[J], 2010, 195(11): 3605

10 Yu Y T, Zhu J H. *Journal of the Electrochemical Society*[J], 2018, 165(5): 297

11 Ebrahimifar H. *Oxidation of Metals*[J], 2019, 91(3): 417

12 Rabbani F, Ward L P, Strafford K N. *Oxidation of Metals*[J], 2000, 54(1-2): 139

13 Qi Q, Liu Y, Huang Z R. *Scripta Materialia*[J], 2015, 109: 56

14 Jo K H, Kim J H, Kim K M *et al*. *International Journal of Hydrogen Energy*[J], 2015, 40(30): 9523

15 Zare R, Sharifi H, Saeri M R *et al*. *Journal of Alloys and Compounds*[J], 2019, 801: 520

16 Qi Q, Wang L J, Liu Y *et al*. *Corrosion Science*[J], 2018, 143: 292

17 Imai Y, Nishi Y. *Journal of the Japan Institute of Metals*[J], 1962, 26(6): 375

18 Shi R, Wang Z, Yang P *et al*. *Corrosion Science*[J], 2014, 88: 101

19 Luo L, Zou L, Schreiber D K *et al*. *Scripta Materialia*[J], 2016, 114: 129

20 Stanislowski M, Froitzheim J, Niewolak L *et al*. *Journal of Power Sources*[J], 2007, 164(2): 578

21 Yuan Y, Cui Y R, Wu K T *et al*. *Journal of Polymer Research*[J], 2014, 21(2): 366

成分设计优化TiC/Hastelloy复合材料的抗氧化性能

齐　倩[1]，王鲁杰[2]，宋晓杰[1]

(1. 山东科技大学 材料科学与工程学院，山东 青岛 266590)

(2. 中国科学院兰州化学物理研究所 固体润滑国家重点实验室，甘肃 兰州 730000)

摘　要：TiC/Hastelloy复合材料是极具应用前景的中温固体氧化物燃料电池连接体材料，而抗氧化性能是影响其应用的关键性能之一。通过无压反应渗透工艺分别制备出含有50vol%和58vol%金属基体的TiC/Hastelloy复合材料。高金属含量使复合材料中的Cr含量增加，促进连续Cr_2O_3氧化层的形成，抑制Ni和Ti原子的外扩散，进而优化复合材料的抗氧化性能。氧化膜中Ti和Ni的氧化物含量降低，复合材料的氧化增重由2.03 mg·cm^{-2}降低到0.55 mg·cm^{-2}。同时，为了抑制Cr挥发，在含有58vol%金属基体的TiC/Hastelloy复合材料中引入Co。在氧化过程中，Co和金属基体中的Fe在Cr_2O_3氧化层中具有较快的扩散速率，可以在Cr_2O_3氧化层外侧原位形成$CoFe_2O_4$层。

关键词：固体氧化物燃料电池；连接体；TiC/Hastelloy复合材料；抗氧化性能

作者简介：齐　倩，女，1989年生，博士，讲师，山东科技大学材料科学与工程学院，山东 青岛 266590，电话：0532-80691739，E-mail：skd995891@sdust.edu.cn